ANALYSIS OF THE INTERPLANETARY EVENTS OBSERVED BY ULYSSES BETWEEN 5 MAY 2002 AND 11 MAY 2002

NEDELIA ANTONIA POPESCU , CRISTIANA DUMITRACHE

Astronomical Institute of Romanian Academy
Str. Cutitul de Argint 5, 40557 Bucharest, Romania
Email: nedelia@aira.astro.ro, crisd@aira.astro.ro

Abstract. In this paper we try to quantify the evolution of solar wind structures, and we analyze the boundaries and the morphology of the interplanetary events registered by the *Ulysses* spacecraft between 5 May 2002 and 11 May 2002. The presence of an magnetic cloud (MC), inside an extended ICME that starts on 5 May 2002 until 9 May 2002, and a spectacular stream interaction region (SIR), between 9 May 2002 and 11 May 2002, is underlined by a number of characteristic signatures regarding the magnetic field, velocity, temperature and density of plasma, together with plasma composition and charge states signatures.

Key words: heliosphere – interplanetary mass ejections – stream interaction regions.

1. INTRODUCTION

The structures and dynamical processes inside the heliosphere are driven by the variable conditions in the solar corona (as function of heliographic coordinates and time), together with the solar wind and the magnetic field embedded in it. The solar transients, such as coronal mass ejections, shocks, as well as the stream interaction regions produce additional dynamical processes. After decades of observations, the study of the two main large-scale spatial structures of the solar wind, the interplanetary coronal mass ejections (ICMEs) and the stream interaction regions (SIRs), still represent important issues. Both these large-scale structures can produce shocks, generate or accelerate energetic particles, and cause effects on the magnetic activity of the Earth and even of other planets from the Solar System. A key element for a successful space weather forecast is represented by the prediction of how these structures evolve radially, following their pass from the Sun through the interplanetary space.

The coronal mass ejections (CMEs) have the origins from closed magnetic field regions in the solar corona and are ejected from the solar atmosphere. CMEs transport large amount of plasma and magnetic flux into interplanetary space (Gosling, 1996; Hundhausen, 1999). The CMEs that propagate through the Solar System can be observed in the interplanetary space as interplanetary coronal mass ejections (Richardson and Cane, 1995; Zurbuchen and Richardson, 2006).

ICMEs can be characterized by a sum of signatures such as helium abundance enhancements, ion/electron temperature depression, strong magnetic fields, low plasma beta, low magnetic field variance, counterstreaming suprathermal (> 60 eV) electrons, counterstreaming energetic protons ($>\sim 20$ keV), characteristic field rotations consistent with flux ropes, different heavy ion composition from the solar wind. These signatures can be or cannot be simultaneously fulfilled (Richardson and Cane, 1995; Zurbuchen and Richardson, 2006).

In comparison with other solar missions that provide baseline ecliptic plane observations (*i.e.*, *Helios 1* and *2*, *IMP-8*, *ACE* and *Wind*), one of the most important achievements of *Ulysses* mission was to collect data on ICMEs along the entire range of heliolatitudes. For the first time the characteristics of these transient events were determined at high heliolatitudes too, due to *Ulysses* exceptionally orbit over the poles of the Sun.

Launched on six of October 1990, the ESA/NASA *Ulysses* mission was in a 6.2-year period orbit of the Sun, inclined at 80.2^o to the solar equator, with perihelion at 1.34 AU and aphelion at 5.4 AU. For the first time, *Ulysses* mission delivered in-situ data from extremely high heliolatitudes, above the solar poles, within the inner heliosphere. In this way the 3D-survey of the heliosphere was obtainable for a long period, exactly 18.7 years of operations.

Ebert *et al.* (2009), Du *et al.* (2010), and Richardson (2014) provided catalogs of ICMEs observed in-situ by *Ulysses* mission. These catalogs were compiled by means of similar identification schemes that considered, besides the basic criterion of the abnormally low proton temperature, additional signatures of the ICME magnetic field and plasma parameters such as: enhanced magnetic field strength, low plasma beta ($\beta < 0.2$), enhanced alpha to proton ratio, smooth rotation in the magnetic field vector (for magnetic cloud detection), bi-directional electrons. Richardson (2014) additionally used in his study the plasma compositional anomalies relative to the composition of the ambient solar wind.

A subset of the ICMEs is represented by the magnetic clouds (MC) that are supposed to be large interplanetary flux ropes (Burlaga, 1988). In-situ spacecraft observations of the solar wind identified the magnetic clouds as special regions that present certain characteristics. Magnetic clouds are defined at 1 AU by the following criteria: a) the magnetic field direction rotates smoothly through a large angle during an interval of the order of one day; b) the magnetic field strength inside the magnetic cloud is higher than in the average solar wind; c) the proton temperature is depressed inside the magnetic cloud (Klein and Burlaga, 1982; Burlaga, 1991).

Liu *et al.* (2005) obtained lists of ICMEs from *Helios 1* and *2*, *Wind*, *ACE*, and *Ulysses* observations, using only the features of enhanced helium abundances, and depressed proton temperatures, the results contributing to the study of the ICME radial evolution from 0.3 AU to 5.4 AU. Also, Wang, Du, and Richardson (2005) com-

bined the criterion of low proton temperature with the signatures of the ICME magnetic field and plasma parameters in an attempt to identify and characterize ICMEs observed by *Helios 1* and *2*, *PVO*, *ACE*, and *Ulysses*.

Due to the Sun rotation, fast and slow streams originating from different sources can collide and interact with each other. In this way, the formation and evolution of stream interaction regions (SIRs) can be explained. The SIRs can be recognized by the presence of compression in the rising-speed portion of the slow stream, the rarefaction in the trailing part of the fast stream, and pressure ridge at the stream interface (SI). When the flow pattern emanating from the Sun is comparatively time stationary, these compression regions form spirals in the solar equatorial plane that corotate with the Sun, producing the corotating interaction region (CIR). The pressure wave that results from the collision of the streams is steepening with radial distance, and eventually produces shocks, a pair of forward-reverse shocks being sometimes encountered. Compression and shocks can heat the plasma within the SIR, this thing giving rise to an increase of the temperature.

In this paper we analyze the morphology of the interplanetary events, registered by the *Ulysses* spacecraft between 5 May 2002 and 11 May 2002, and determined the boundaries of these events. The presence of an extended ICME, that lasts for five days starting with 5 May 2002, along with the existence of a spectacular stream interaction region (SIR), between 9 May – 11 May 2002, are pointed up using multiple signatures regarding the magnetic field, velocity, temperature and density of plasma, as well as plasma composition signatures.

2. THE DATA SETS AND PARAMETERS UNDER USE

On 5 May 2002, *Ulysses* was situated at 3.364 AU and 46.1^o North heliographic latitude relative to the Sun. For the study of the events between 5 May – 11 May 2002, we considered data from three instruments onboard of *Ulysses*: VHM (magnetometer) that provides the magnetic field components (Br, Bt, Bn) and magnitude B, with 1-h averaged solar wind data; SWOOPS (Solar Wind Plasma Experiment), with 1-h averaged solar wind data; SWICS (Solar Wind Ion Composition Instrument), with time resolution of 3-hours.

The solar wind parameters used in our study are: the proton bulk velocity Vp; the proton number density Np; the density ratio of α particle to proton (N_α/Np); the magnetic field vector in RTN coordinates system of the spacecraft (Br, Bt, Bn), and the magnitude B; the plasma β, that represents the ratio of thermal to magnetic pressure $\beta = Np \cdot k_B \cdot Tp/[B^2/(8 \cdot \pi)]$; the total protons pressure, expressed as the sum of the kinetic and magnetic pressures $Pt = Np \cdot k_B \cdot Tp + B^2/(8 \cdot \pi)$, where k_B is the Boltzman constant.

The three axes of the RTN reference frame are as follows: R indicates the radial Sun-spacecraft anti-sunward direction, T is the tangential direction obtained from the cross-product between the solar rotation axis and R, and N is the normal direction which completes the frame.

In the catalogs of Liu *et al.* (2005), Ebert *et al.* (2009), Du *et al.* (2010), and Richardson (2014), the ICME that starts on 5 May 2002 can also be found, but with different boundaries and description.

In the process of the tracking back to the Sun of the studied ICME, we used the CDAW CMEs catalogue (http://cdaw.gsfc.nasa.gov/CME-list) for the identification of the solar source.

3. THE BOUNDARIES DETECTION AND MORPHOLOGY OF THE INTERPLANETARY EVENTS

The interplanetary events between 5 May – 11 May 2002 are analyzed based on a set of characteristics regarding their magnetic field, velocity, temperature, density, and plasma composition using in-situ data recorded from VHM, SWOOPS, and SWICS instruments on board of *Ulysses* (see Section 2).

By means of classical identification criteria of ICMEs (He^{++} abundance enhancement, low kinetic temperature, low velocity), plasma dynamics signatures, and plasma composition signatures (anomalies of abundance and charge state of heavy ion species), we carry out a detailed description and analysis of the ICME and SIR.

Figure 1 presents the interplanetary magnetic field and plasma data for the studied interplanetary events (ICME and SIR), for a period of nine days starting with day of the year DOY 123. From top to bottom are presented the magnetic field components (Br, Bt, Bn) and the magnitude of the magnetic field (B); the proton density (Np) and the ratio Tp/T_{exp}; the solar wind proton velocity (Vp).

The expected temperature T_{exp} follows the condition $Tp/T_{exp} < 0.5$ for ICMEs, being calculated with the relations of Lopez (1987), for distances exceeding 1 AU:

$$T_{exp}(10^3 K) = \begin{cases} \frac{(0.031v-5.1)^2}{r^{0.7}}, v < 500 \\ \frac{(0.51v-142)}{r^{0.7}}, v \geq 500 \end{cases}$$

Thus, the horizontal line in the second panel of Figure 1 represents the threshold of $Tp/T_{exp} = 0.5$. The vertical lines assign the detected boundaries, that will be described in the next sections.

In the sequel we discuss the ICME and SIR separately, presenting in detail their morphology and the boundary detection.

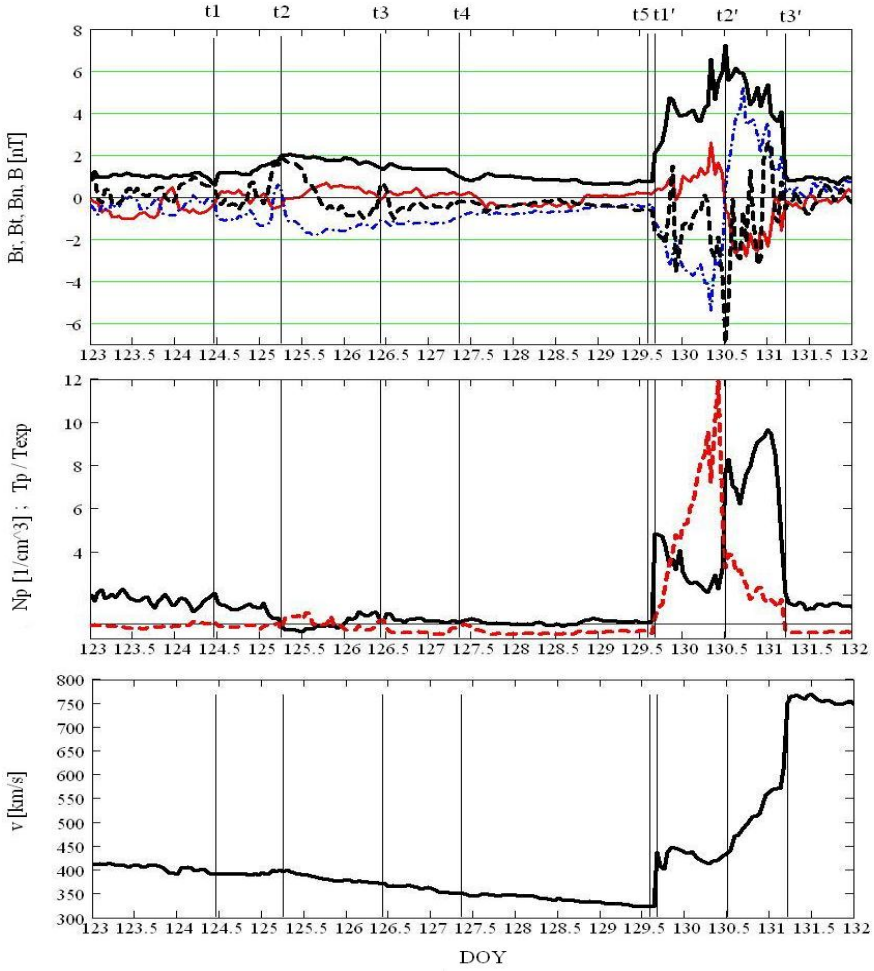

Fig. 1 – Interplanetary magnetic field and plasma data for an interval of nine days starting with DOY 123. Vertical lines assign the boundaries of the ICME and SIR. First panel: magnetic field components and magnitude: Br (thin line), Bt (dash–dotted line), Bn (dashed line), B (thick line); Second panel: proton number density Np (dashed line), Tp/T_{exp} temperatures ratio (thick line); Third panel: solar wind bulk speed Vp.

3.1. THE ICME ON 5 MAY – 9 MAY 2002

The first part of the analyzed ICME presents the features of a magnetic cloud: the magnetic field rotates smoothly through a large angle, the strength of the magnetic field is higher than in the average solar wind, and the temperature is lower than that in the average solar wind (Burlaga, 1995).

From top to bottom, the four panels of Figure 2 present the magnetic field

components (Br, Bt, Bn) and the magnitude of the magnetic field (B), the plasma β, the alpha to proton ratio N_α/Np, the bulk velocity Vp, and the total proton pressure Pt (see Section 2), for a period of seven days starting with DOY 123.

In Figure 2, the first vertical line points the arrival of a weak forward shock at $t1 = 124.45$, and the beginning of the sheath that developed until $t2 = 125.25$. The typical characteristics of the sheath (*i.e.*, enhanced B magnitude, high levels of magnetic field fluctuations, plasma beta, and mass density) are present along this period of time.

A first part of the ICME presents the characteristics of an MC, lasting from $t2 = 125.25$ to $t4 = 127.35$, followed by a second part which shows a non-cloud ICME structure (until $t5 = 129.585$).

The presence of a strong magnetic field magnitude B, with a relatively smooth rotations in Bn (field rotations consistent with flux ropes for MC) can be observed in the top panel of Figure 2. For plasma beta in ICMEs, a threshold of 0.2 is used, representing a value used by various authors (Foullon *et al.*, 2007; Lepping *et al.*, 2009). The plasma β values are positioned under the threshold of 0.2 for the entire period of the analyzed ICME (Figure 2, panel 2).

Usually, the enhanced N_α/Np ratio above $0.06 - 0.08$ represents an important signature of the ICME presence (Richardson and Cane, 2004; Neugebauer and Goldstein, 1997; von Steiger and Richardson, 2006). Such a characteristic can be observed in the case of the studied MC (Figure 2, panel 3). A declining profile of velocity Vp, from about 400 km s^{-1} to 325 km s^{-1}, and the total pressure Pt enhancement represent other specific features of an MC (panels 4 and 5, Figure 2).

Within the MC, two substructures are revealed by means of the minimum variance analysis (MVA) (Sonnerup and Cahill, 1967; Bothmer and Schwenn, 1998), applied for 1 minute resolution data from the *Ulysses*/VHM instrument. The MC1 and MC2 substructures start at $t2 = 125.25$ to $t3 = 126.42$, and $t3 = 126.42$ to $t4 = 127.35$, respectively.

In Figure 3 we present the magnetic field components in the local magnetic coordinates system (Bxc, Byc, Bzc) (corresponding to the maximum variance, intermediate variance and minimum variance directions, respectively), obtained from the minimum variance analysis (for a detailed description, see Dumitrache, Popescu, and Oncica, 2011). Figure 3 shows the hodogram of the magnetic field components for the MC1 (with squares) and MC2 (with stars), in the Bxc – Byc plane.

Considering the fulfilled conditions of a stronger than ambient magnetic field magnitude B, low proton temperature, low plasma beta, and enhanced alpha to proton density ratio we conclude that this event has the well defined features of a long lasting magnetic cloud, in its first part, as well as the features of a non-cloud ICME in the second part.

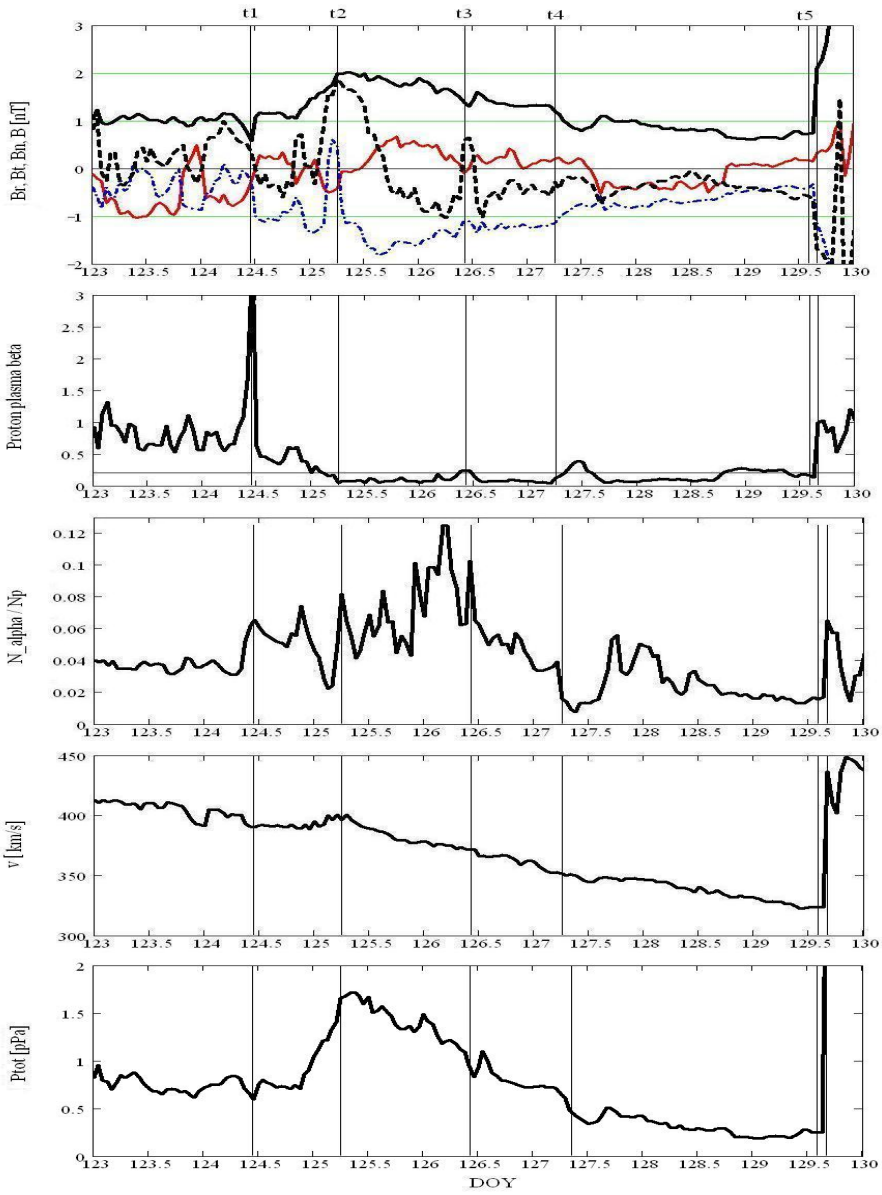

Fig. 2 – The in-situ observations of ICME. The data cover an interval of seven days, starting with DOY 123. First panel: magnetic field components Br (thin line), Bt (dash-dotted line), Bn (dashed line), and magnitude B (thick line); Second panel: proton plasma β; Third panel: N_α/Np ratio; Fourth panel: solar wind bulk velocity Vp; Fifth panel: total proton pressure Pt.

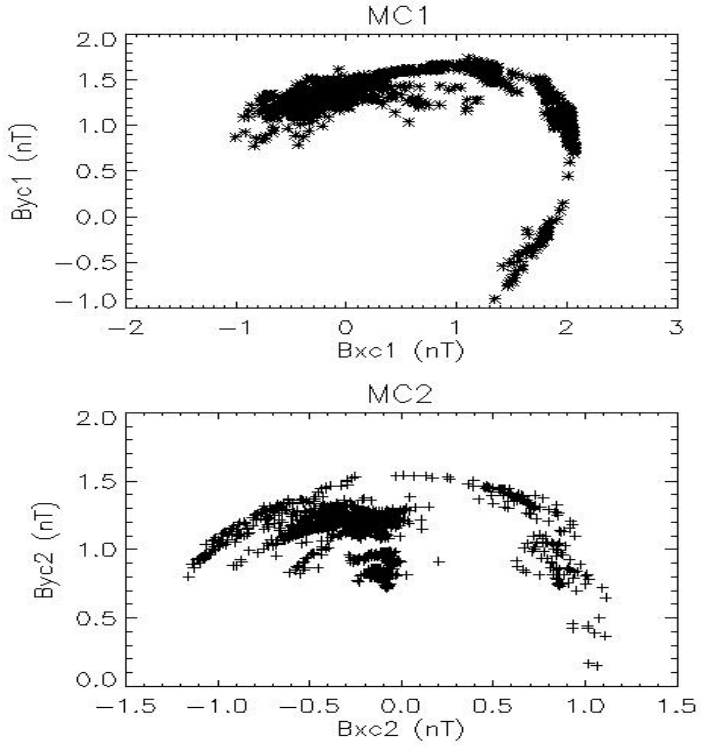

Fig. 3 – Magnetic field components in local magnetic coordinates obtained from the minimum variance analysis: the hodogram for the MC1 (with squares) and MC2 (with stars), in the Bxc-Byc plane.

3.2. STREAM INTERACTION REGION ON 9 MAY – 11 MAY 2002

For the SIR's determination the following criteria are usually used: the proton bulk velocity increase; the proton temperature enhancement; an increase and then a decrease of proton number density; a pile-up of the dynamical pressure $Pdyn$ with decreases at two sides; the change of entropy, defined as $ln(Tp^{3/2}/Np)$, that represents an indication of the sources of different plasmas; the deviation of the flow (Jian *et al.*, 2008; Jian *et al.*, 2009).

In Figure 4, from top to bottom, are presented for an interval of three days the magnetic field components (Br, Bt, Bn) and magnitude (B); proton density Np , proton temperatures Tp, and bulk velocity Vp; the entropy; total proton pressure Pt.

In the case of SIRs, a pair of forward-reverse shocks can be found once in a while. Within the SIRs the plasma can be heated by the compression and shocks, this thing giving rise to an increase of the temperature. By means of the criteria previously mentioned we determined the boundaries of the SIR on 9 May – 11 May 2002 as

$t1' = 129.666$ (9 May, 15:59 UT) and $t3' = 131.208$ (11 May, 05:00 UT). These two boundaries represent forward and reverse shocks, and they were confirmed by the data from Gosling and Forsyth (http://www.sp.ph.ic.ac.uk/Ulysses/shocklist.txt).

In Figure 4, second panel, the forward shock and the reverse shock are depicted, along with the stream interface (SI) at $t2' = 130.5$. The increase of the velocity from ~ 450 km s^{-1}, on DOY 129, to ~ 768 km s^{-1}, on DOY 131, produces a greater compression of the plasma interface region and leads to higher pressures (see Figure 4, panel three and four). The resulting stresses directed outward from the stream interface (SI) will produce faster large amplitude waves and shocks. The peak pressures are positioned at the interfaces between the slow and fast wind (see Figure 4, panel four).

Concluding, the SI is present at the peak of Pt, where usually Tp and Vp increase and Np begins to drop after a plasma compression region.

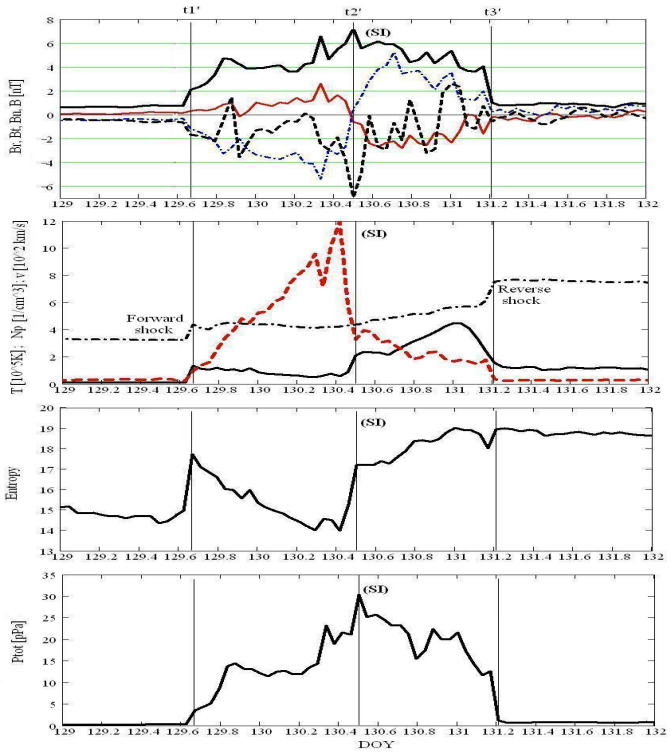

Fig. 4 – The in-situ observations of SIR, for an interval of three days starting with DOY 129. First panel: magnetic field components and magnitude: Br (thin line), Bt (dash-dotted line), Bn (dashed line), and B (thick line); Second panel: proton temperature Tp, proton number density Np, velocity Vp; Third panel: the entropy: Fourth panel: total proton pressure Pt.

From the polarity changes of Br and Bt, that can be seen on the 1 minute resolution data from the *Ulysses*/VHM instrument, we observed that multiple heliospheric current sheet (HCS) crossings are encountered in the interval DOY 130.48 - DOY 130.495, and DOY 130.58 - DOY 130.595, at both sides of the stream interface (DOY 130.5).

4. SOLAR WIND COMPOSITION AND CHARGE STATE ANALYSIS

The analysis of the plasma composition signatures (*i.e.*, the anomalies of abundance and charge state of heavy ion species) represents an additional tool for the ICME boundaries confirmation.

A study of the compositional differences between the fast and slow streams from *Ulysses* data was performed by Geiss *et al.* (1995). The conclusion was that coronal composition is influenced by the chromospheric ionization and transport processes, and the intensity of these processes is correlated with the temperature in the corona. Each ionic charge state has a specific freeze-in point, for a given speed, temperature, and density profile. Burgi and Geiss (1986) established that O^{7+}/O^{6+} ratio is freezing in closer than one solar radius from the photosphere. As a general result, the O^{7+}/O^{6+} ratio contains a coronal "indent" of the source region for the solar wind.

The relation $O^{7+}/O^{6+} > 1$ is a practical marker of material from a hot solar source, and it corresponds to a coronal temperature of 2×10^6 K degrees (Henke *et al.*, 2001; Zurbuchen *et al.*, 2003). In the case of ICME, $O^{7+}/O^{6+} > 1$ represents an important condition that have to be fulfilled (Neugebauer and Goldstein, 1997), being especially encountered in MCs (Henke *et al.*, 1998). Many authors considered in their studies smaller values as thresholds, such as $O^{7+}/O^{6+} = 0.6$ (Gopalswamy *et al.*, 2013), or $O^{7+}/O^{6+} = 0.7$ (Burlaga *et al.*, 2001).

The ICME threshold of $Fe/O = 0.25$ results from the relation stated by Ipavich *et al.* (1986): $(Fe/O)_{CME}/(Fe/O)_{photosphere} > 5$, where $(Fe/O)_{photosphere}$ = 0.05. Finally, according to Lepri and Zurbuchen (2004), the optimum threshold value for the mean Fe charge state is considered $< Q_{Fe} >= 11$, greater values being indicators for the presence of ICMEs.

In Figure 5, the time evolution of O^{7+}/O^{6+}, C^{6+}/C^{5+}, Fe/O charge states ratios, and average Fe charge states, $< Q_{Fe} >$ are presented. In each panel, the horizontal lines represent the specific thresholds of these charge states ratios and average Fe charge state (*i.e.*, $O^{7+}/O^{6+} = 0.6$, $C^{6+}/C^{5+} = 3$, $Fe/O = 0.25$, and $< Q_{Fe} >= 11$). In the studied interval for the ICME (between $t2 = 125.25$ and $t5 = 129.585$), we observe that all these quantities exceed the above mentioned thresholds, high values being accomplished for the non-cloud ICME interval ($O^{7+}/O^{6+} = 1.25$,

$< Q_{Fe} >$ =13.5, $Fe/O = 0.55$, and even $C^{6+}/C^{5+} = 18.7$).

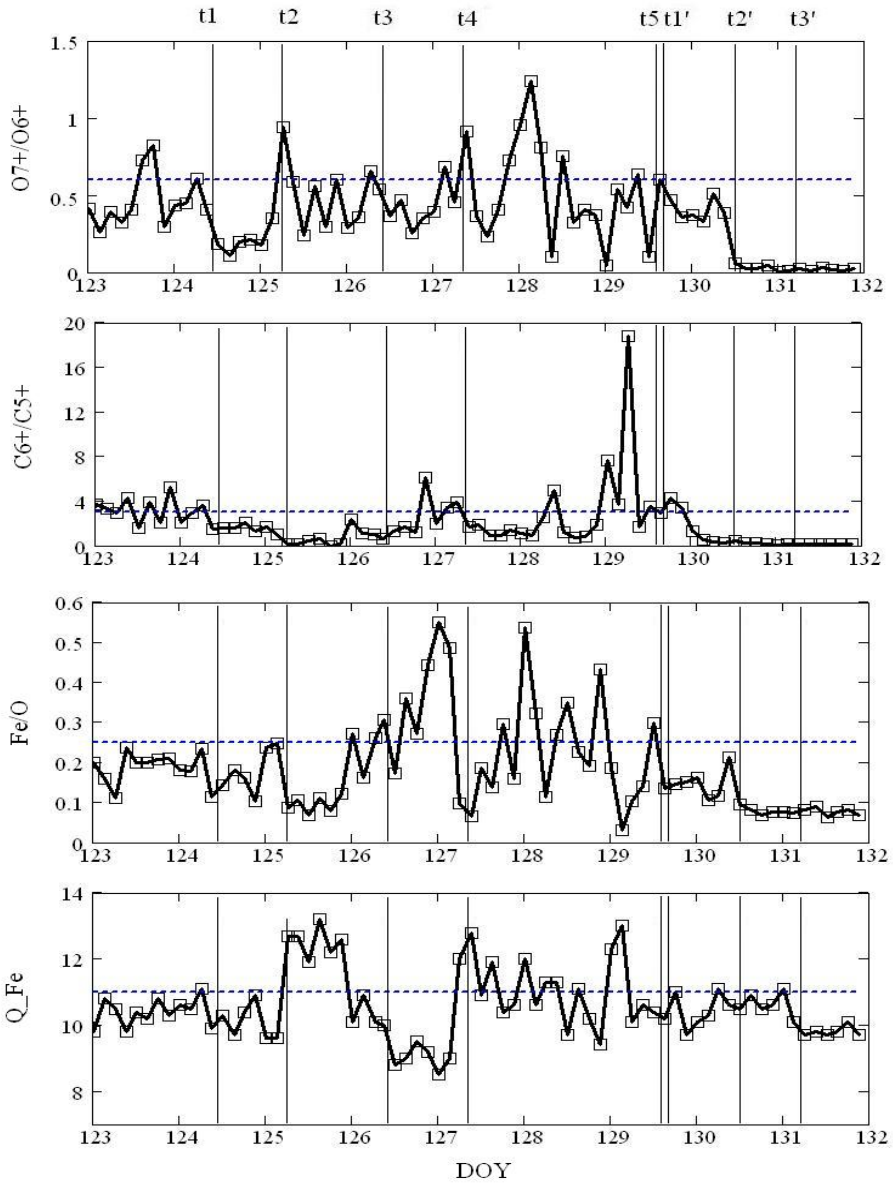

Fig. 5 – The distributions of O^{7+}/O^{6+}, C^{6+}/C^{5+}, Fe/O, and $< Q_{Fe} >$, for an interval of nine days starting with DOY 123.

5. TRACKING BACK TO THE SUN OF THE ICME

The occurrence day of the solar CME has been computed using a linear approach and a graphical method for the tracking back of the ICME to the Sun (for a detailed description, see Dumitrache, Popescu, and Oncica, 2011). As we already mention above, on 5 May 2002 *Ulysses* was situated at 3.364 AU and 46.1^o north heliographic latitude relative to the Sun. The ICME started at DOY 125.25 and had the velocity Vp = 397.3 km s^{-1}.

Thus, the computed day of occurrence for the solar counterpart is DOY 110.506. Around this date, the CDAW CMEs catalogue presents 2 solar sources registered by The Solar and Heliospheric Observatory (SOHO) satellite (with SOHO/EIT and SOHO/LASCO C2 instruments):

– a Halo CME1 on 21 April 2002 (DOY = 111), that starts at 0h 43min UT, ends at 02h 38min, and has a velocity v = 2393 km s^{-1}, coming from the active region NOAA9906;

– a CME2 on 24 April 2002 (DOY = 114), that starts at 21h 46min UT, ends at 22h 01min, with a velocity v = 576 km s^{-1}, coming from the active region NOAA9912, under a certain position angle $PA = 313^o$ (PA = Position Angle measured counter-clockwise from Solar North in degrees).

In Table 1 are presented the results obtained for the estimation of the propagation in the interplanetary space for CME1 and CME2. The results on the CMEs' arrival at *Ulysses* indicate the CME2 as the solar counterpart event, whose arrival is on DOY 126.06 at *Ulysses*, this one being closer to the day of the ICME starting, DOY 125.25. Figure 6 presents the CME2 source considered to be the solar counterpart of the ICME event on *Ulysses*. In the left and right panels the SOHO/EIT and SOHO/LASCO C2 observations are presented.

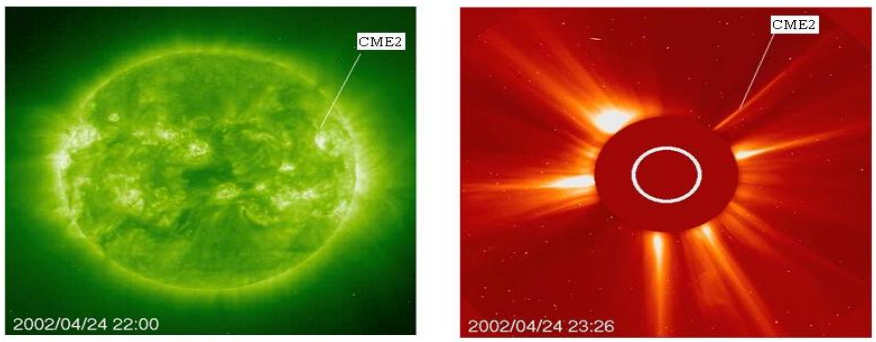

Fig. 6 – The CME2 solar counterpart of the ICME event on *Ulysses*. Left panel: SOHO/EIT observations; Right panel: SOHO/LASCO C2 observations.

Table 1

Estimation of CMEs propagation

CME	Data	CME speed (km s^{-1})	CME's start DOY	CME's arrival DOY
Halo CME1	21 April 2002, 00:43 UT	2393	111.04	113.47
CME2	24 April 2002, 21:46 UT	576	114.96	126.06

6. CONCLUSIONS

In this paper we present two successive interplanetary events that have been register between 5 May – 11 May 2002 at *Ulysses*. Using in-situ data recorded from VHM, SWOOPS, and SWICS instruments on board of *Ulysses*, these events have been analyzed based on their magnetic field, velocity, temperature, and density characteristics, as well as on their plasma composition signatures (the anomalies of abundance and charge states). Regarding the boundaries and the morphology of the studied events, we determined for the ICME between 5 May – 9 May 2002 the characteristics of a long lasting magnetic cloud that exists in the first part (from $t2 = 125.25$ to $t4 = 127.35$), as well as the features of a non-cloud ICME in the second part (from $t4 = 127.35$ to $t5 = 129.585$). The MC consists of two substructures revealed by means of the minimum variance analysis (MVA) applied for 1 minute resolution data from the *Ulysses*/VHM instrument. Also, as result of the tracking back to the Sun of the studied ICME, we determined the CME2 as the solar counterpart. This CME had a velocity of v = 576 km s^{-1}, and came from the active region NOAA9912, under a certain position angle $PA = 313^o$.

In the period between 9 May – 11 May 2002, we determined a stream interaction region (SIR) that starts on $t1' = 129.666$ and stops on $t3' = 131.208$. This SIR presents a pair of forward-reverse shocks, an increasing velocity profile, a density rising and entropy changing in the acceleration phase. At the stream interface (SI) the peak of total pressure Pt is encountered, together with the steep increasing of Tp and entropy, and a sharp density drop. Also, multiple crossings of the heliospheric current sheet are encountered in the vicinity of the stream interface.

Acknowledgements. This paper was presented at the International Symposium "The Astronomer Nicolae Donici – 140 years after the birth", Bucharest, 8th September 2014. Regarding the data from *Ulysses*, we acknowledge the SWOOPS and SWICS Teams, and also the National Space Science Data Center and the Principal Investigator, Dr. A. Balogh from Imperial College, London, UK, for the VHM data. The CME catalog uses data from SOHO, being generated and maintained at the CDAW Data Center, by NASA and the Catholic University of America, in cooperation with the Naval Research Laboratory.

REFERENCES

Bothmer, V., and Schwenn, R.: 1998, *Annales Geophysicae* **16**, 1.
Burgi, A., and Geiss, J.: 1986, *Solar Phys.* **103**, 347.
Burlaga, L.F.: 1988, *J. Geophys. Res.* **93**, 7217.
Burlaga, L.F.E.: Physics of the Inner Heliosphere II. Particles, Waves and Turbulence, XI, Springer-Verlag Berlin Heidelberg New York. Also Physics and Chemistry in Space, volume 21, 2, p. 1-22, 1991.
Burlaga, L.F.: Interplanetary Magnetohydrodynamics, Oxford Univ. Press, New York, 89-114, 1995.
Burlaga, L.F., Skoug, R.M., Smith, C.W., Webb, D.F., Zurbuchen, T.H., Reinard, A.: 2001 *J. Geophys. Res.* **106**, 20957.
Dumitrache, C., Popescu, N.A., and Oncica, A.: 2011, *Solar Phys.* **272**, 137.
Du,D., Zuo, P.B., and Zhang, X.X.: 2010, *Solar Phys.* **262**, 171.
Ebert, R.W., McComas, D.J., Elliott, H.A., Forsyth, R.J., Gosling, J.T.: 2009, *J. Geophys. Res.* **114**, 1109.
Foullon, C., Owen, C.J., Dasso, S., Green, L.M., Dandouras, I., Elliott, H.A., Fazakerley, A.N., Bogdanova, Y.V., and Crooker, N.U.: 2007, *Solar Phys.* **244**, 139.
Geiss, J., Gloeckler, G., von Steiger, R.: 1995, *Space Sci. Rev.* **72**, 49.
Gopalswamy, N., Makela, P., Akiyama, S., Xie, H., Yashiro, S., Reinard, A. A.: 2013, *Solar Phys.* **284**, 17.
Gosling, J. T.: 1996, *Annual Rev. Astron. Astrophys.* **34**, 35.
Henke, T.,Woch, J., Mall, U., Livi, S., Wilken, B., Schwenn, R., Gloeckler, G., von Steiger, R., Forsyth, R.J., Balogh, A.: 1998, *Geophys. Res. Lett.* **25**, 3465.
Henke, T., Woch, J., Schwenn, R., Mall, U., Gloeckler, G., von Steiger, R., Forsyth, R.J., Balogh, A.: 2001, *J. Geophys. Res.* **106**, 10597.
Hundhausen, A.J.: 1999, The Many Faces of the Sun: A Summary of the Results From NASA's Solar Maximum Mission, edited by K. T. Strong *et al.*, p. 143, Springer, New York.
Ipavich, F.M., Galvin, A.B., Gloeckler, G., Dovestadt, D., Klecker, B.: 1986, *J. Geophys. Res.* **91**, 4133.
Jian, L.K., Russell, C.T., Luhmann, J.,G., Skoug, R.M., Steinberg, J.T.: 2008, *Solar Phys.* **249**, 85.
Jian, L.K., Russell, C.T., Luhmann, J.G., Galvin, A.B., MacNeice, P.J.: 2009, *Solar Phys.* **259**, 345.
Klein, L.W., and Burlaga, L.F.: 1982, *J. Geophys. Res.* **87**, 613.
Lepping, R.P., Narock, T.W., Wu, C.-C. : 2009, *Ann. Geophys.* **27**, 1295.
Lepri, S.T., and Zurbuchen, T.H. : 2004, *J. Geophys. Res.* **109**, 1112.
Liu, Y., Richardson, J. D., Belcher, J. W.: 2005, *Planet. Space Sci.* **53**, 3.
Lopez, R.E.: 1987, *J. Geophys. Res.* **92**, 11189.
Neugebauer, M., and Goldstein, R.: 1997, *Geophys. Monogr. Ser.* **99**, 245.
Richardson, I.G., and Cane, H.V.: 1995, *J. Geophys. Res.* **100**, 23397.
Richardson, I.G., and Cane, H.V.: 2004, *J. Geophys. Res.* **109**, 9104.
Richardson, I.G.: 2014, *Solar Phys.* **289**, 3843.
Sonnerup, B.U.O. and Cahill, L.J.,Jr.: 1967, *J. Geophys. Res.* **72**, 171.
von Steiger, R., and Richardson, J.D.: 2006, *Space Sci. Rev.* **123**, 111.
Wang, C., Du, D., Richardson, J.D.: 2005, *J. Geophys. Res.* **110**, 10107.
Zurbuchen, T., Fisk, L.A., Lepri, S.T., von Steiger, R.: 2003, The Composition of Interplanetary Coronal Mass Ejections, in M. Velli, R. Bruno and F. Malara (eds.), Solar Wind Ten, AIP Conf. Proc. 679, Mellville, N.Y., 604.
Zurbuchen, T.H., and Richardson, I.G.: 2006, *Space Sci. Rev.* **123**, 31.

Received on 20 February 2015